

Supporting Information:

Sequential detection of Fe^{3+} and As^{3+} ions by naked eye through aggregation and dis-aggregation of biogenic gold nanoparticles

*Somasundaram Kaviya and Edamana Prasad **

Department of Chemistry, Indian Institute of Technology Madras, Chennai-600 036, India

Table of content

1. UV-vis spectra and TEM image of AuNPs synthesized at different concentration of extract
2. UV-vis spectra and TEM image of AuNPs at 10^{-6} M of HAuCl_4
3. EDAX profile of biosynthesized AuNPs
4. XRD patterns of biosynthesized AuNPs
5. Zeta potential and size measurements of AuNPs
6. FT-IR spectrum of aqueous pomegranate peel extract
7. UV-vis absorption spectrum of aqueous solution of pomegranate peels extract.
8. UV-vis spectra of AuNP1 and 2 with different metal ions
9. UV-vis spectra of AuNP3 and 4 with different metal ions
10. UV-vis absorption spectra of AuNPs with the addition of different concentration of Fe^{3+} ions
11. TEM image of $\text{Fe}@\text{Au}$ (core @ shell) NPs in the case of AuNP2
12. XRD patterns of biosynthesized AuNPs (1-4) in presence of 10^{-6} M of Fe^{3+}
13. EDAX profile of AuNPs in presence of 10^{-6} M of Fe^{3+}
14. Interference study of AuNPs + Fe^{3+} in the presence of other metal ions (10^{-2} M)
15. DLS measurement of AuNPs upon addition of 10^{-6} M Fe^{3+} ions
16. DLS measurement of AuNP4 upon addition of 10^{-6} M Fe^{3+} ions
17. TEM and SEM images of aggregation of AuNP1 and AuNP2 upon addition of 10^{-6} M of Fe^{3+} ions.
18. TEM and SEM images of aggregation of AuNP1 and AuNP2 upon addition of 10^{-6} M of Fe^{3+} ions.
19. *Logistic* growth fitting for time dependent aggregation of AuNP1-3 upon addition of different concentration of Fe^{3+} ions

- 20.** Liner fitting of observed rate constant vs different concentration of Fe^{3+} ions for AuNP1-3
- 21.** Linear fitting data for AuNP – Fe systems
- 22.** Exponential decay fitting for the time dependent aggregation of AuNP (1-3) - Fe upon addition of different concentration of As^{3+} ions
- 23.** Liner fitting of observed rate constant vs different concentration of As^{3+} ions for AuNP (1-3) –Fe
- 24.** Linear fitting data for AuNP – Fe - As^{3+} system
- 25.** SEM images of dis-aggregation of AuNP (1&2) -Fe upon addition of 10^{-3} M of As^{3+} ions
- 26.** SEM images of dis-aggregation of AuNP (3&4) -Fe upon addition of 10^{-3} M of As^{3+} ions
- 27.** TEM and SEM images of aggregation and disaggregation of AuNP1 in presence of Fe^{3+} (10^{-6} M) and As^{3+} (10^{-3} M) ions.
- 28.** TEM and SEM images of aggregation and disaggregation of AuNP2 in presence of Fe^{3+} (10^{-6} M) and As^{3+} (10^{-3} M) ions.
- 29.** TEM and SEM images of aggregation and disaggregation of AuNP3 in presence of Fe^{3+} (10^{-6} M) and As^{3+} (10^{-3} M) ions.
- 30.** DLS measurement of AuNPs – Fe system upon addition of 10^{-3} M As^{3+} ions
- 31.** DLS measurement of AuNP4 – Fe system upon addition of 10^{-3} M As^{3+} ions
- 32.** XRD patterns of AuNPs-Fe system with the addition of 10^{-3} M of As^{3+} ions
- 33.** Interference study of AuNPs-Fe system with As^{3+} in the presence of other metal ions
- 34.** UV-vis spectra of AuNPs upon addition of tap water

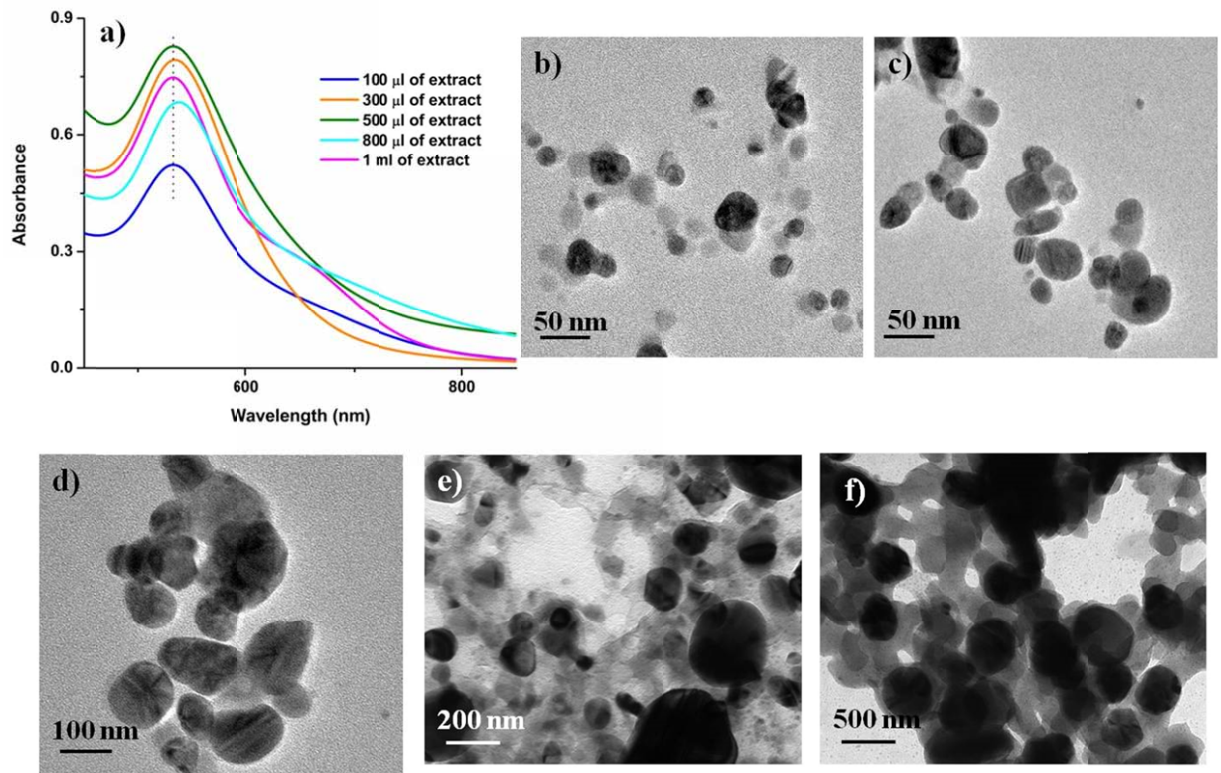


Fig. S1 a) UV-vis spectra and TEM images of AuNPs synthesized (10^{-3} M of HAuCl₄) with the addition of b) 100 µL, c) 300 µL, d) 500 µL, e) 800 µL and f) 1mL of peel extract.

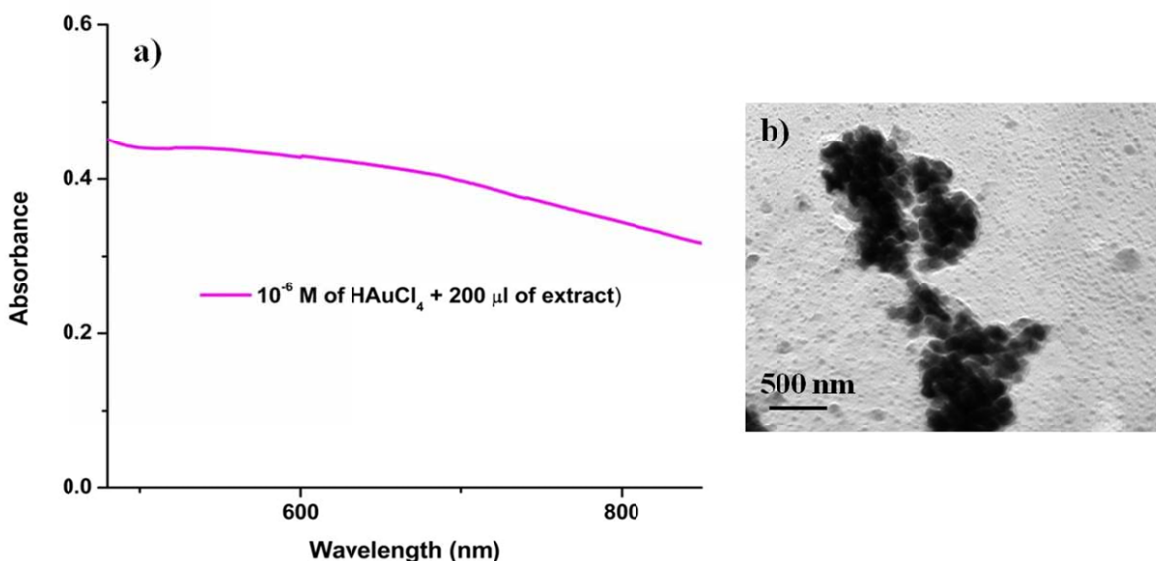


Fig. S2 a) UV-vis absorption spectrum and b) TEM image of AuNPs (200 µL of extract and 10^{-6} M HAuCl₄)

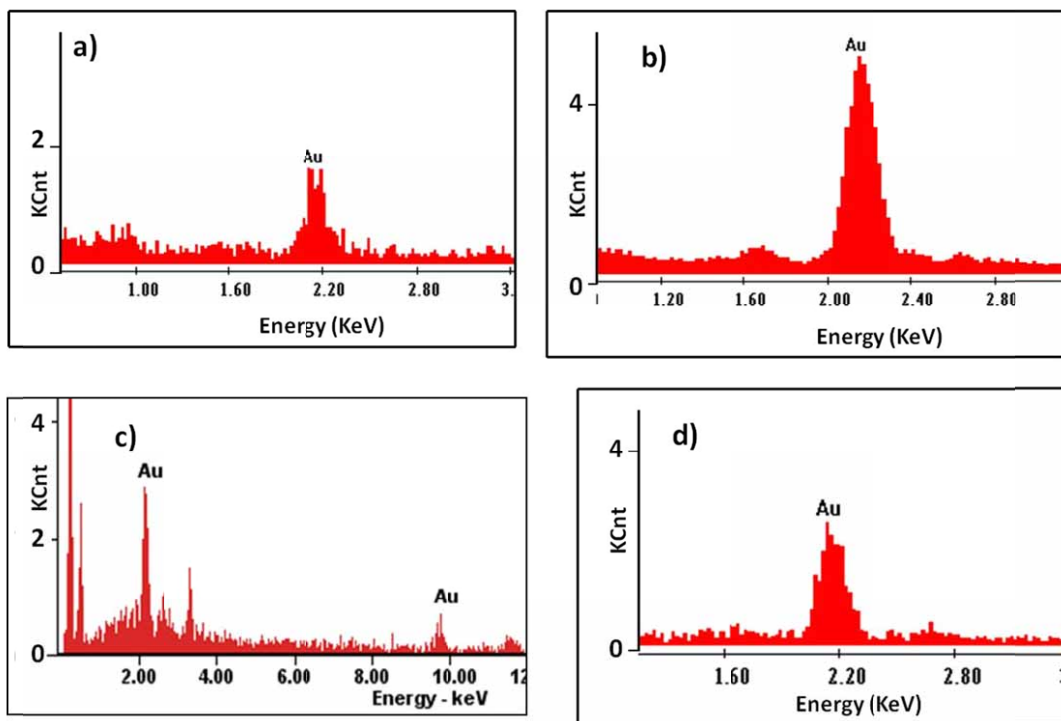


Fig. S3 EDAX profile of pomegranate peel extract stabilized a) AuNP1, b) AuNP2, c) AuNP3 and d) AuNP4.

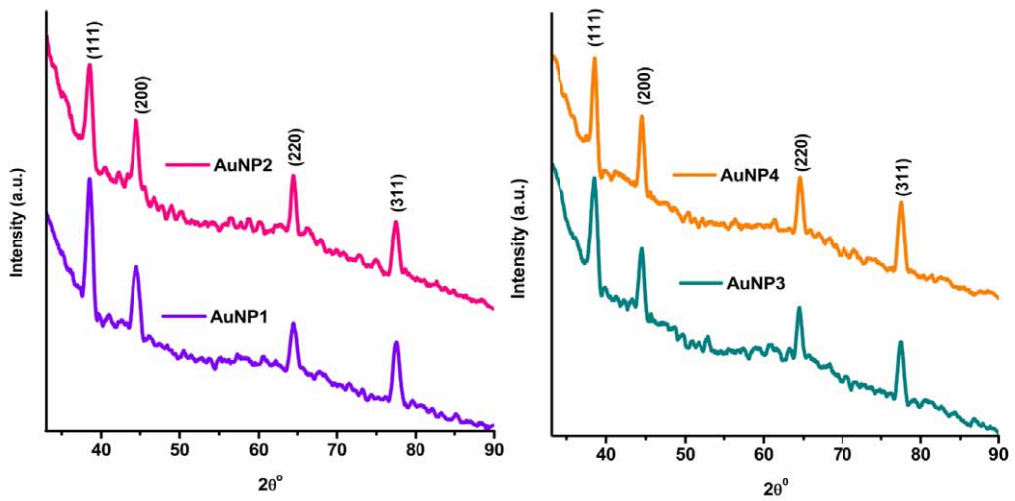


Fig. S4 XRD patterns of biosynthesized AuNPs (1-4).

Table S1 Zeta potential and size measurements of AuNPs

S. No	System	Zeta potential (mV)	Particle Size (nm)
1.	extract	-22.6	-
2.	AuNP2	-18.3	22.91
3.	AuNP3	-19.5	40.51
4.	AuNP4	-21.3	115.20

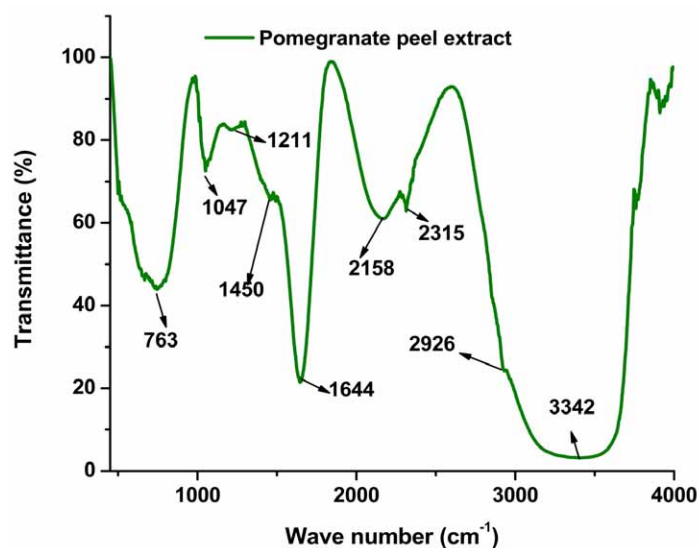


Fig. S5 FT-IR spectrum of aqueous pomegranate peel extract.

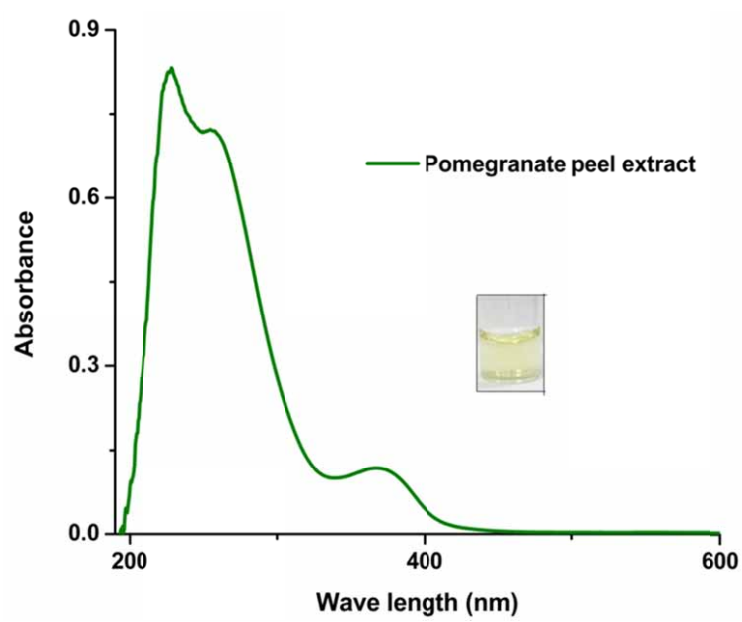


Fig. S6 UV-vis absorption spectrum of aqueous solution of pomegranate peels extract.

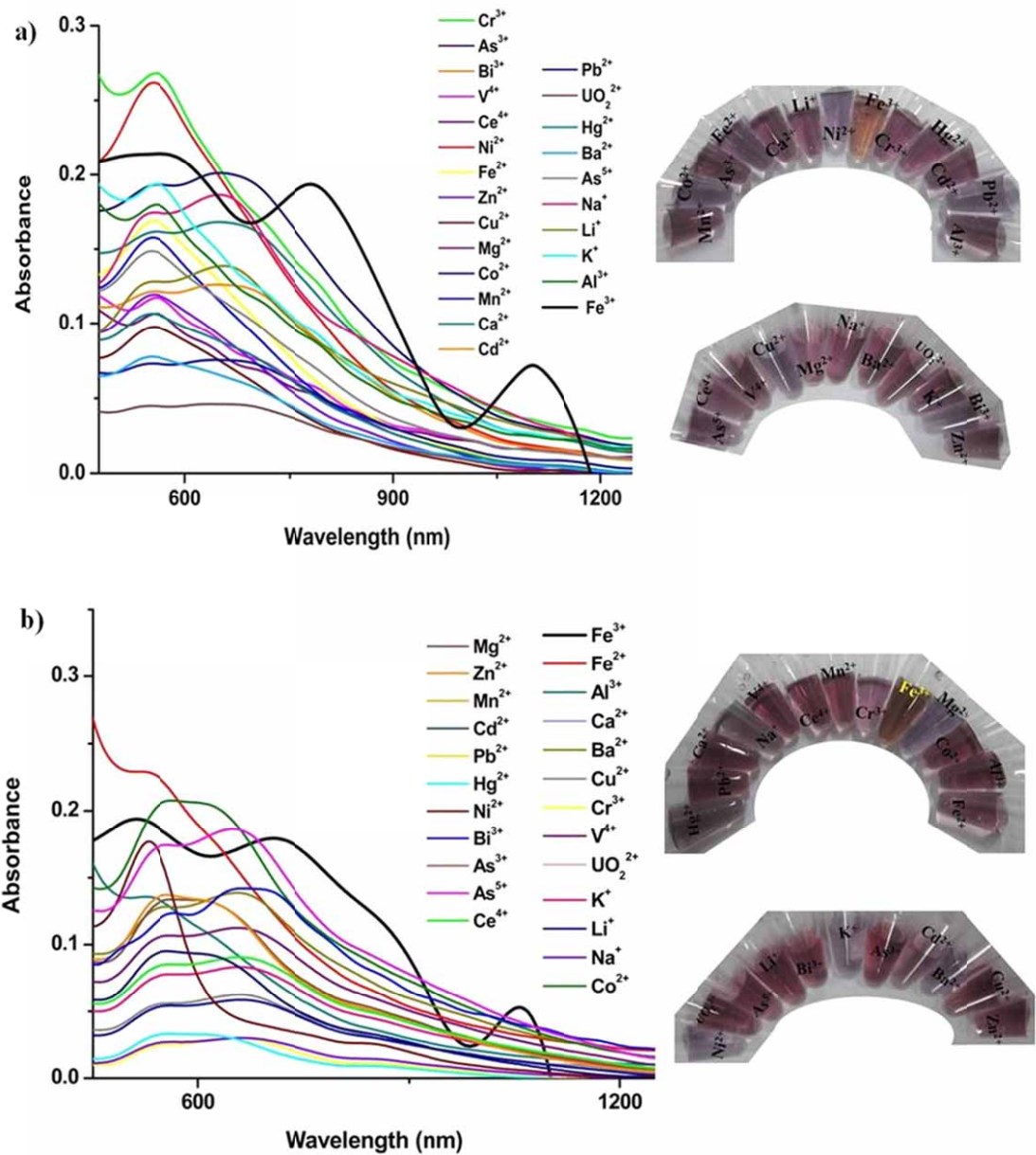


Fig. S7 UV-vis spectra of the a) AuNP1 and b) AuNP2 respectively, upon addition of different metal ions (10^{-2} M) and their corresponding photographic images (right).

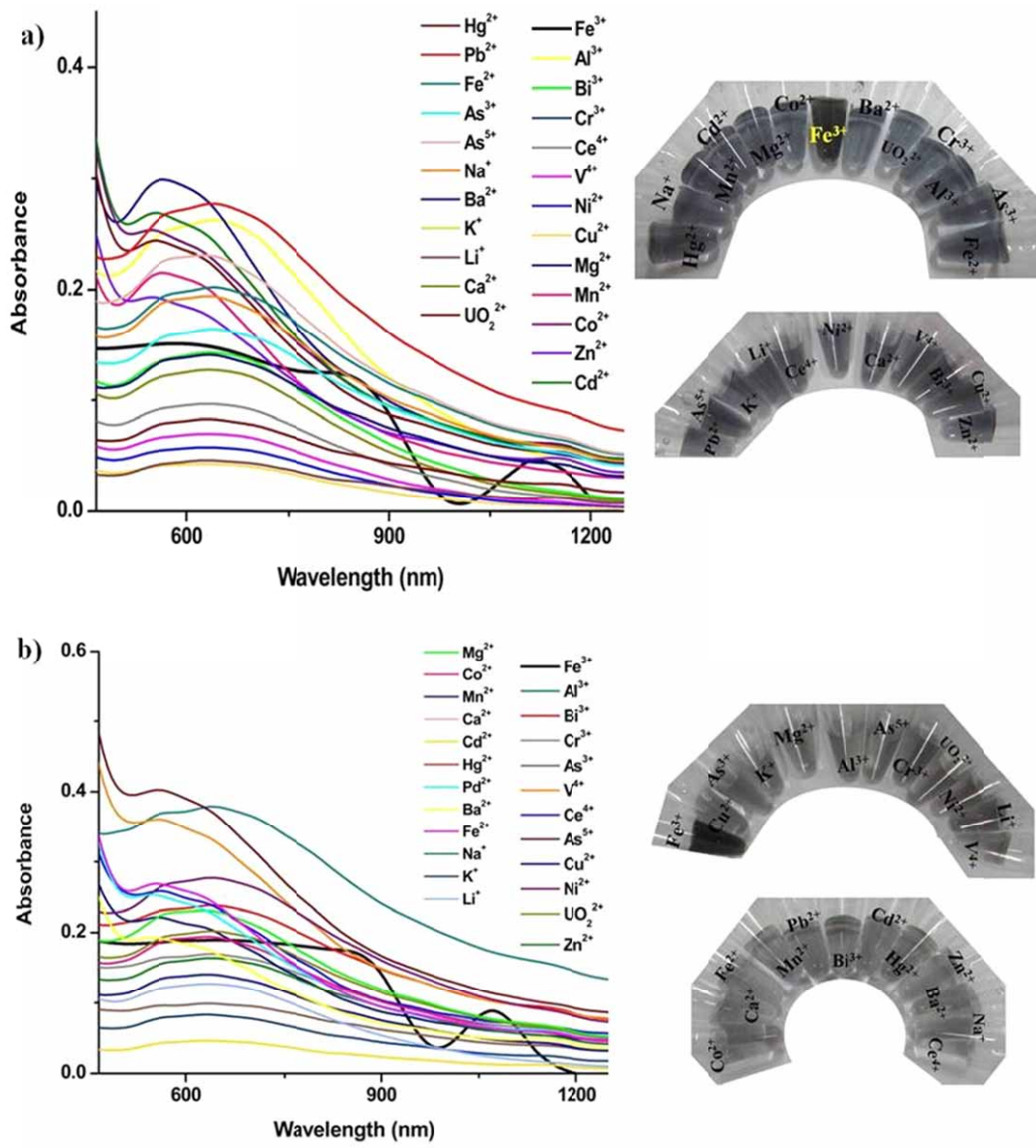


Fig. S8 UV-vis spectra of the a) AuNP3 and b) AuNP4, respectively, upon addition of different metal ions (10^{-2} M) and their corresponding photographic images (right).

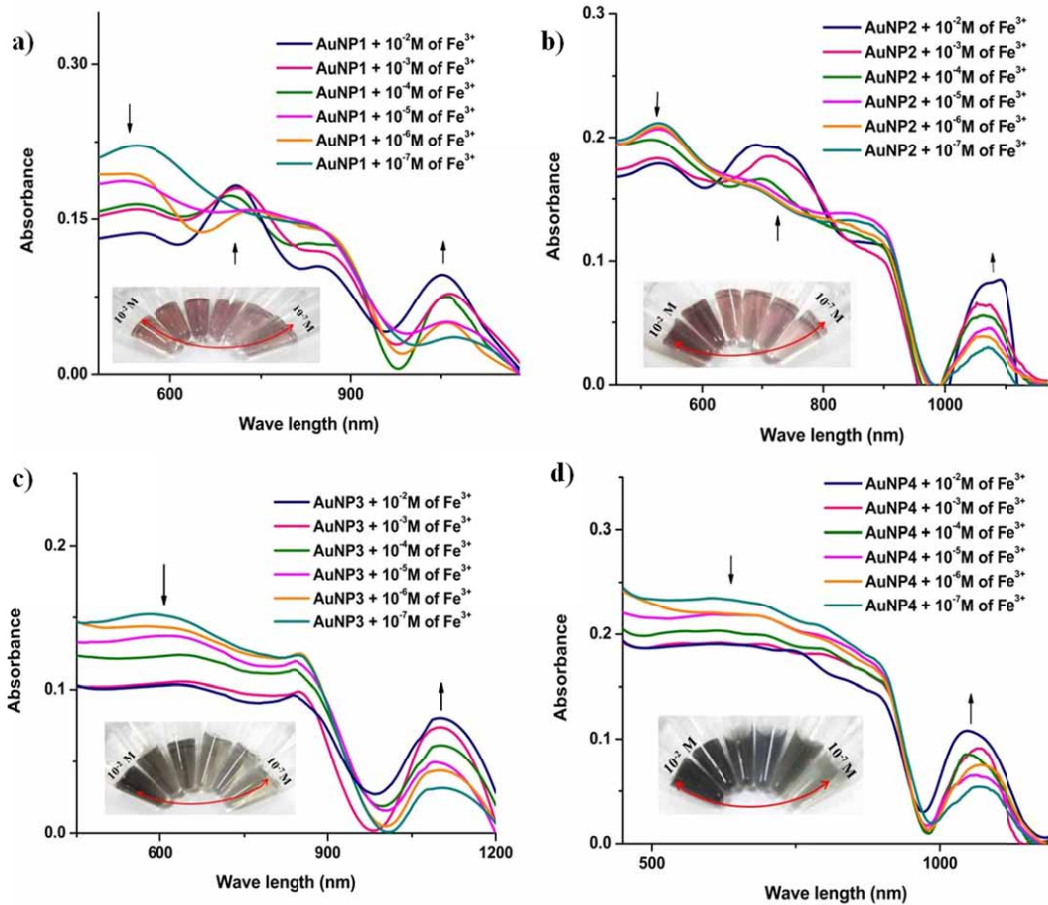


Fig. S9 UV-vis absorption spectra of AuNPs with the addition of different concentration of Fe^{3+} ions. Inset: the corresponding photographic images.

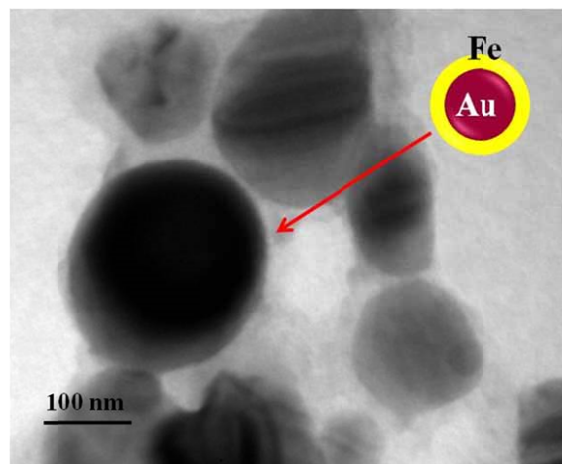


Fig. S10 TEM image shows for the formation of Fe@Au (core @ shell) NPs in the case of AuNP2 in presence of 10^{-6} M of Fe^{3+} ions.

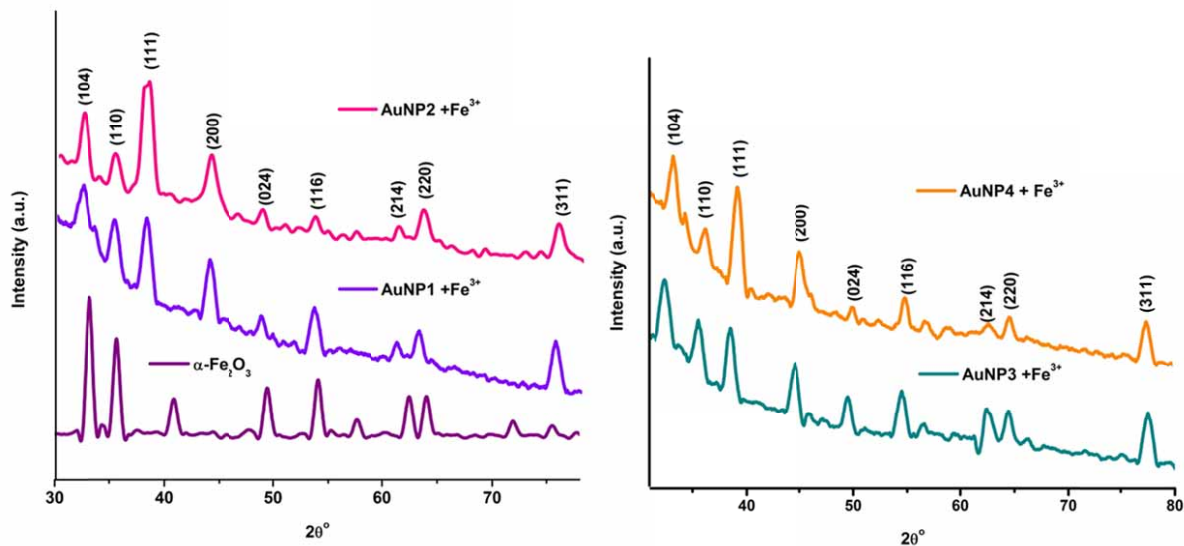


Fig. S11 XRD patterns of biosynthesized AuNPs (1-4) in presence of 10^{-6} M of Fe^{3+} .

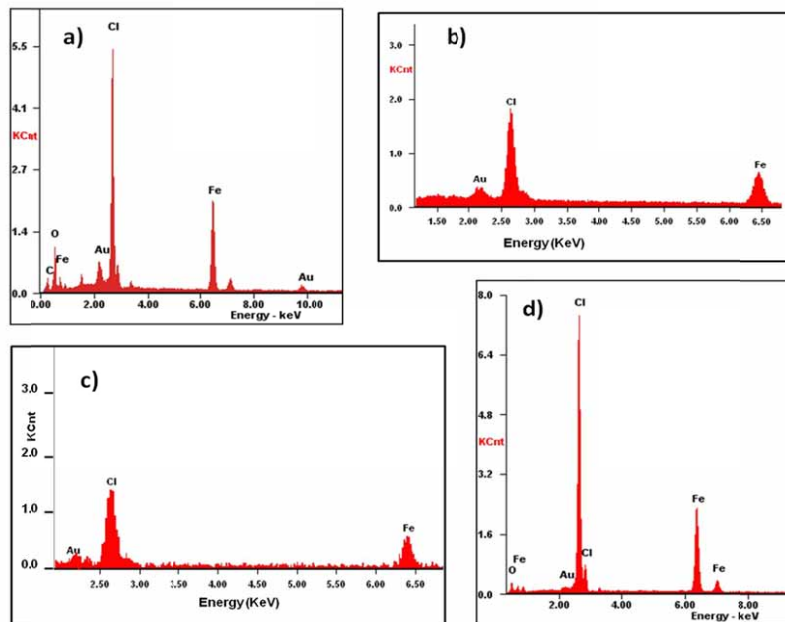


Fig. S12 EDAX profile of pomegranate peel extract stabilized a) AuNP1, b) AuNP2, c) AuNP3 and d) AuNP4 in presence of 10^{-6} M of Fe^{3+} .

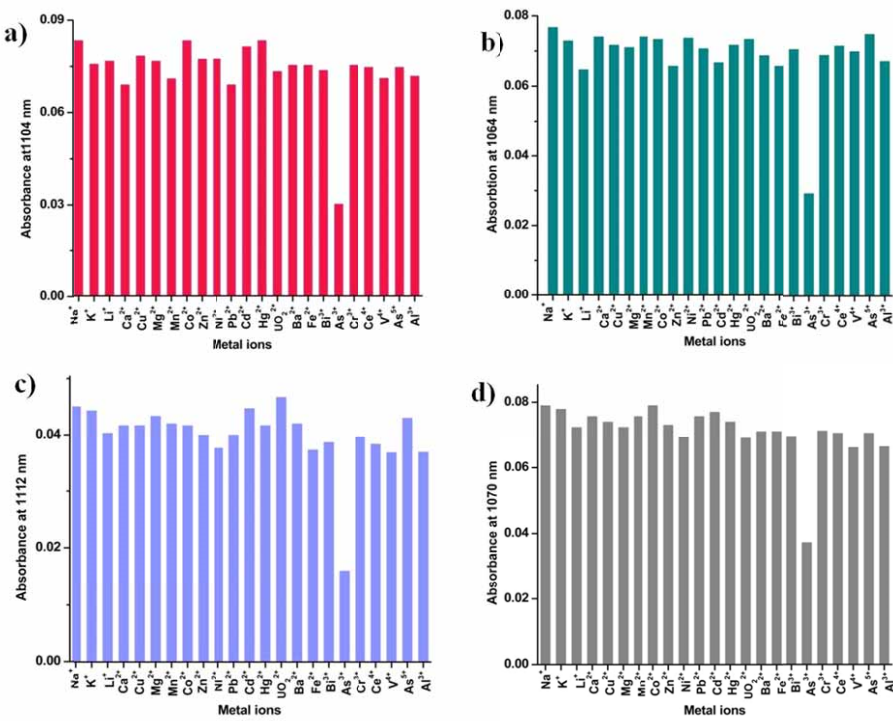


Fig. S13 Interference study of a) AuNP1 b) AuNP2 c) AuNP3 d) AuNP4 and Fe^{3+} in the presence of other metal ions (10^{-2} M).

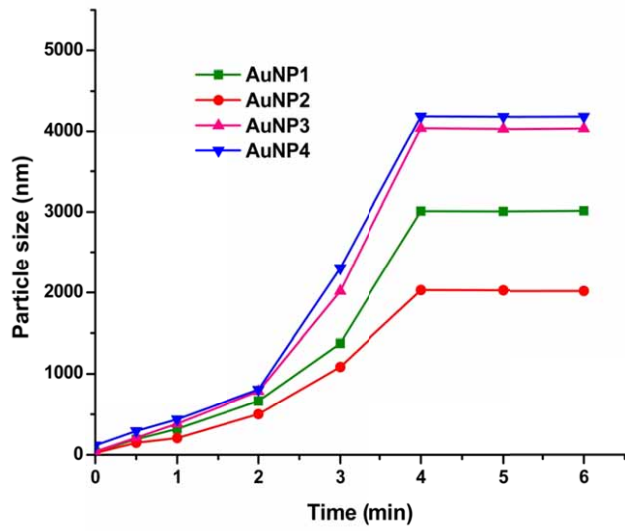


Fig. S14 Time dependent aggregation and change in particle size of AuNPs (1-4) upon addition of 10^{-6} M Fe^{3+} ions by DLS measurement.

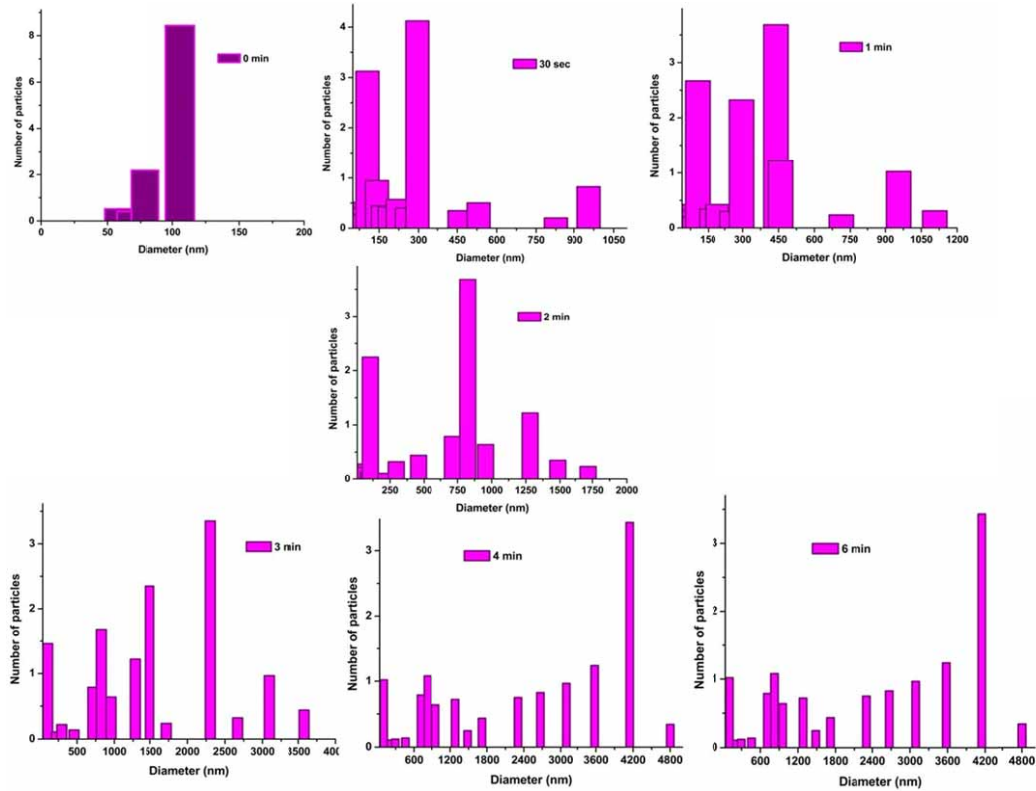


Fig. S15 Time dependent aggregation and change in particle size of AuNP4 upon addition of 10^{-6} M Fe^{3+} ions by DLS measurement.

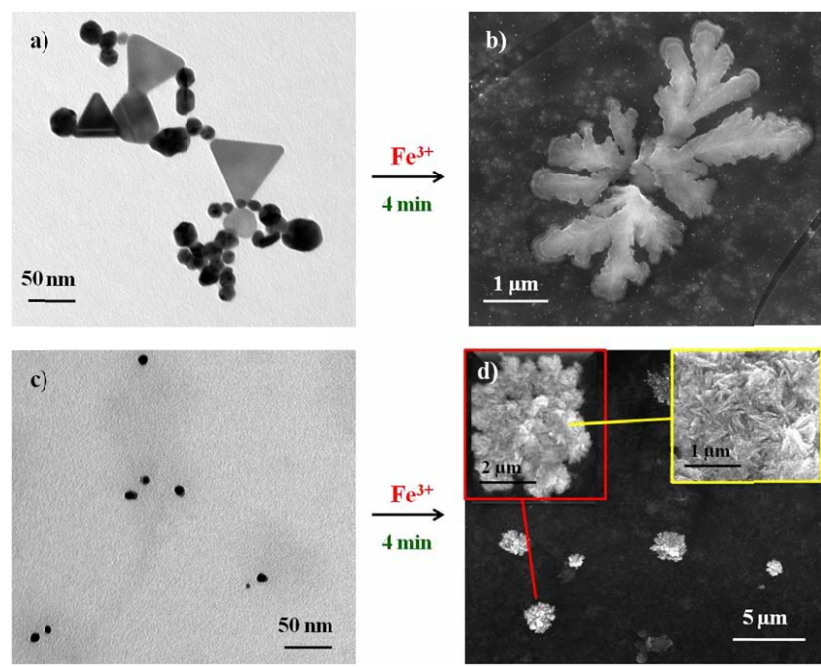


Fig. S16 TEM (a, c) and SEM (b, d) images shows the aggregation of AuNP1 (a) and AuNP2 (c) upon addition of 10^{-6} M of Fe^{3+} ions.

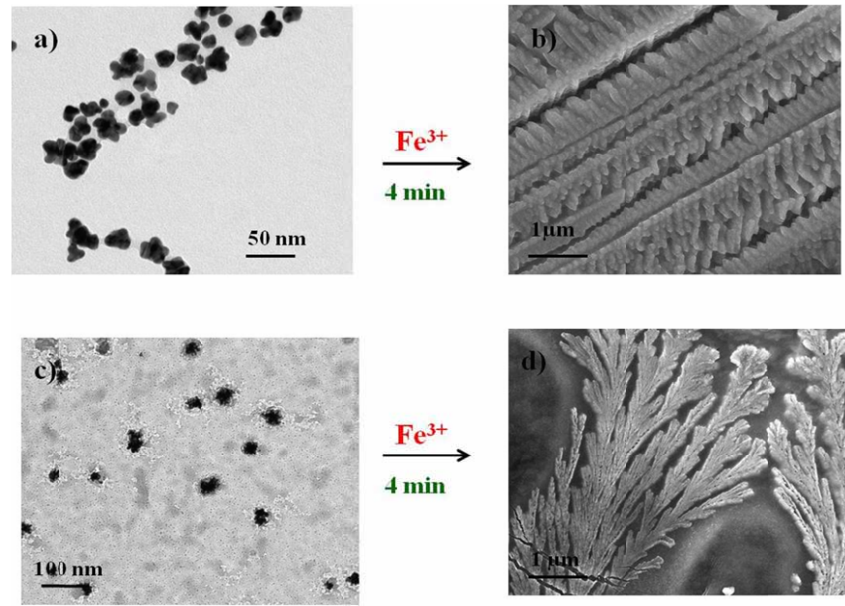


Fig. S17 TEM (a, c) and SEM (b, d) images shows the aggregation of AuNP3 (a) and AuNP4 (c) upon addition of 10^{-6} M of Fe^{3+} ions.

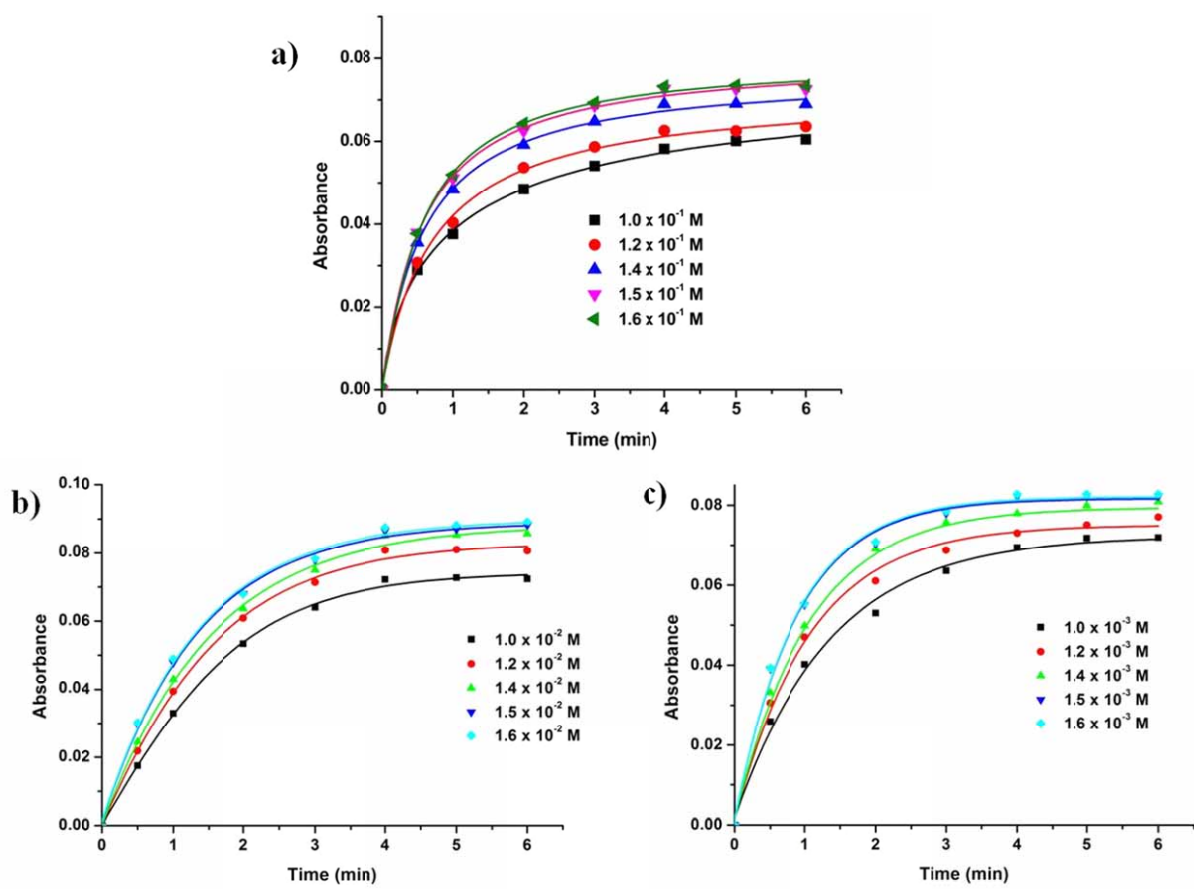


Fig. S18 Logistic growth fitting for time dependent aggregation of a) AuNP1, b) AuNP2 and c) AuNP3 upon addition of different concentration of Fe^{3+} ions.

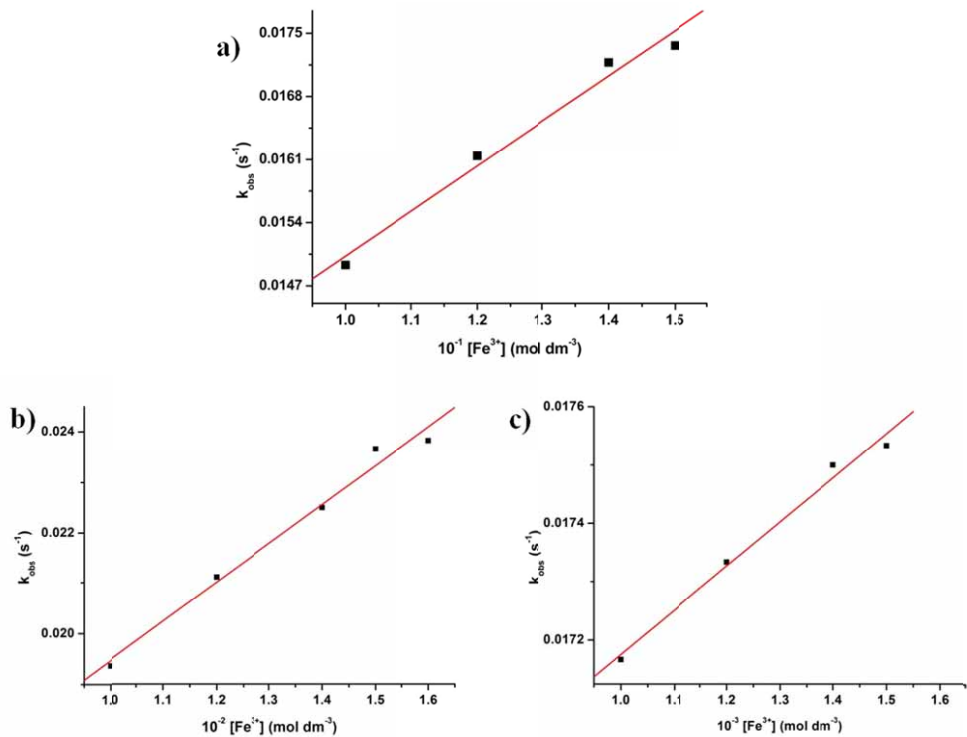


Fig. S19 Liner fitting of observed rate constant vs different concentration of Fe^{3+} ions for a) AuNP1, b) AuNP2 and c) AuNP3.

Table S2 Linear fitting data for AuNP – Fe systems

Using equation $y = a + b \cdot x$ in figure 19

System	Rate constant (k), s^{-1}	Standard error	R^2
Plot a*	5.0×10^{-3}	3.8066E-4	0.9900
Plot b*	7.7×10^{-3}	5.4940E-5	0.9880
Plot c*	7.0×10^{-4}	5.8713E-5	0.9821
Plot d [#]	7.0×10^{-3}	6.23517E-4	0.9900

(Note: * = Plots (1-3) in figure S19 (a-c) and # = insect in figure 5)

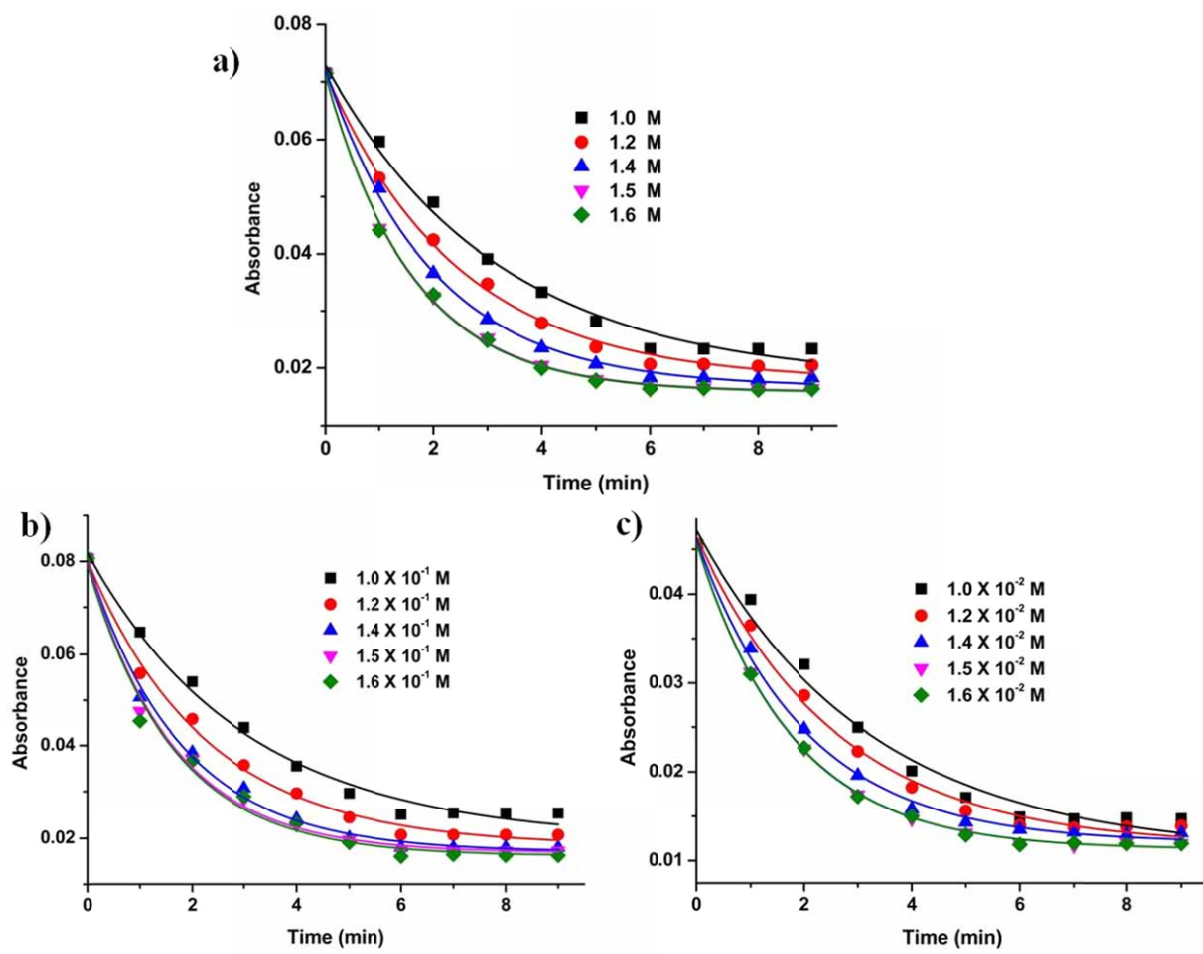


Fig. S20 Exponential decay fitting for the time dependent aggregation of a) AuNP1- Fe b) AuNP2 -Fe and c) AuNP3- Fe upon addition of different concentration of As^{3+} ions.

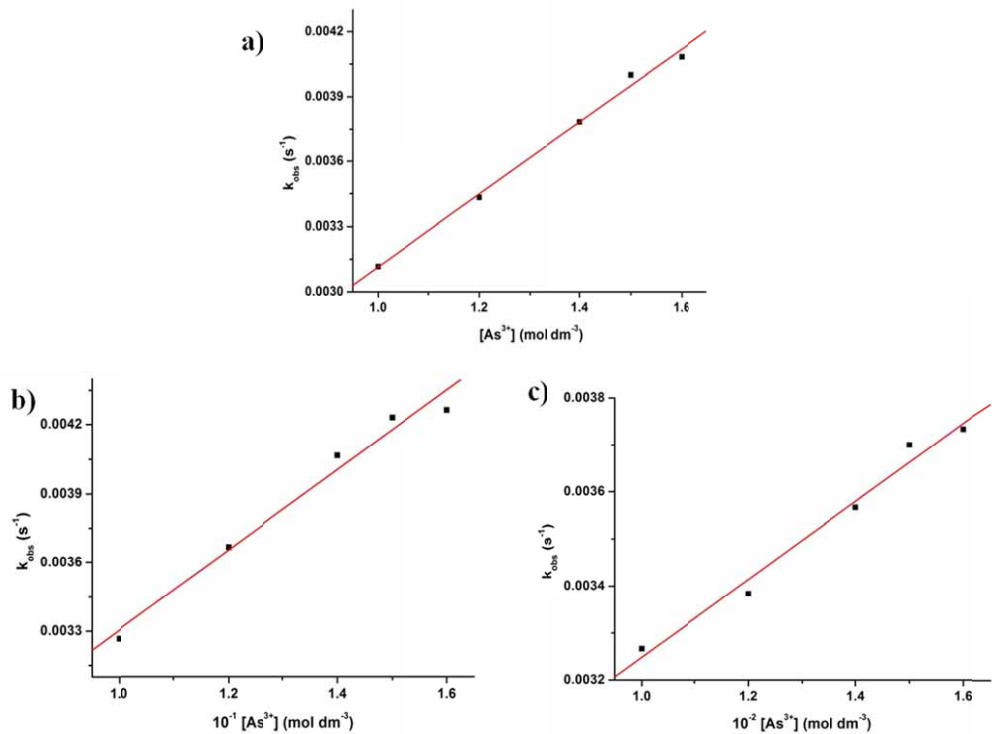


Fig. S21 Liner fitting of observed rate constant vs different concentration of As^{3+} ions for a) AuNP1-Fe, b) AuNP2-Fe and c) AuNP3-Fe.

Table S3 Linear fitting data for AuNP – Fe - As^{3+} system

Using equation $y = a + b \cdot x$ in figure 27

System	Rate constant (k), s^{-1}	Standard error	R^2
Plot a*	1.6×10^{-3}	3.8066E-4	0.9900
Plot b*	1.7×10^{-3}	7.5441E-5	0.9880
Plot c*	8.0×10^{-4}	8.6997E-5	0.9900
Plot d [#]	8.0×10^{-4}	6.23517E-4	0.9900

(Note: * = Plots (1-3) in figure S27 (a-c) and # = insect in figure 7)

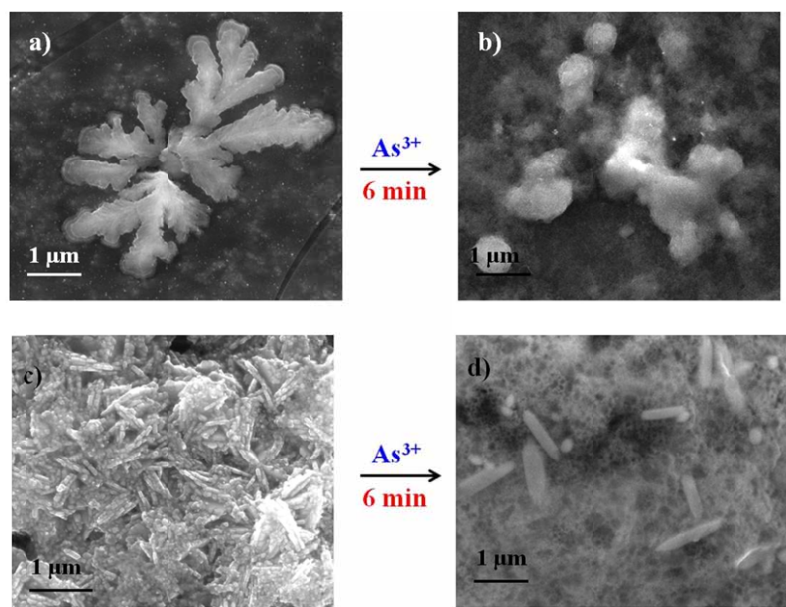


Fig. S22 SEM images showing the dis-aggregation of (a) AuNP1-Fe and (c) AuNP2-Fe upon addition of 10^{-3} M of As^{3+} ions.

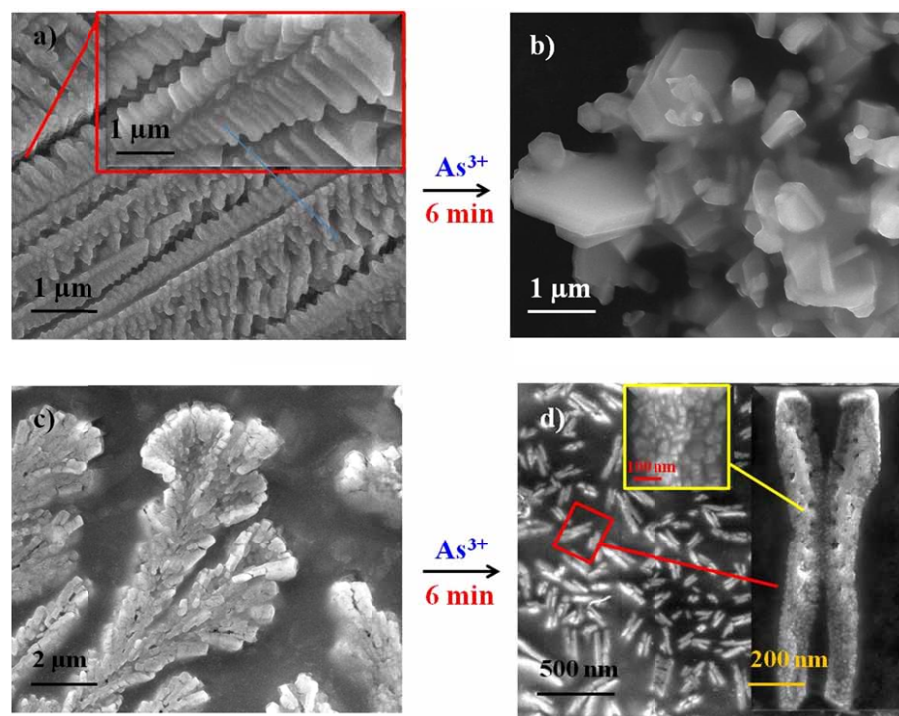


Fig. S23 SEM images showing the dis-aggregation of (a) AuNP3-Fe and (c) AuNP4-Fe upon addition of 10^{-3} M of As^{3+} ions.

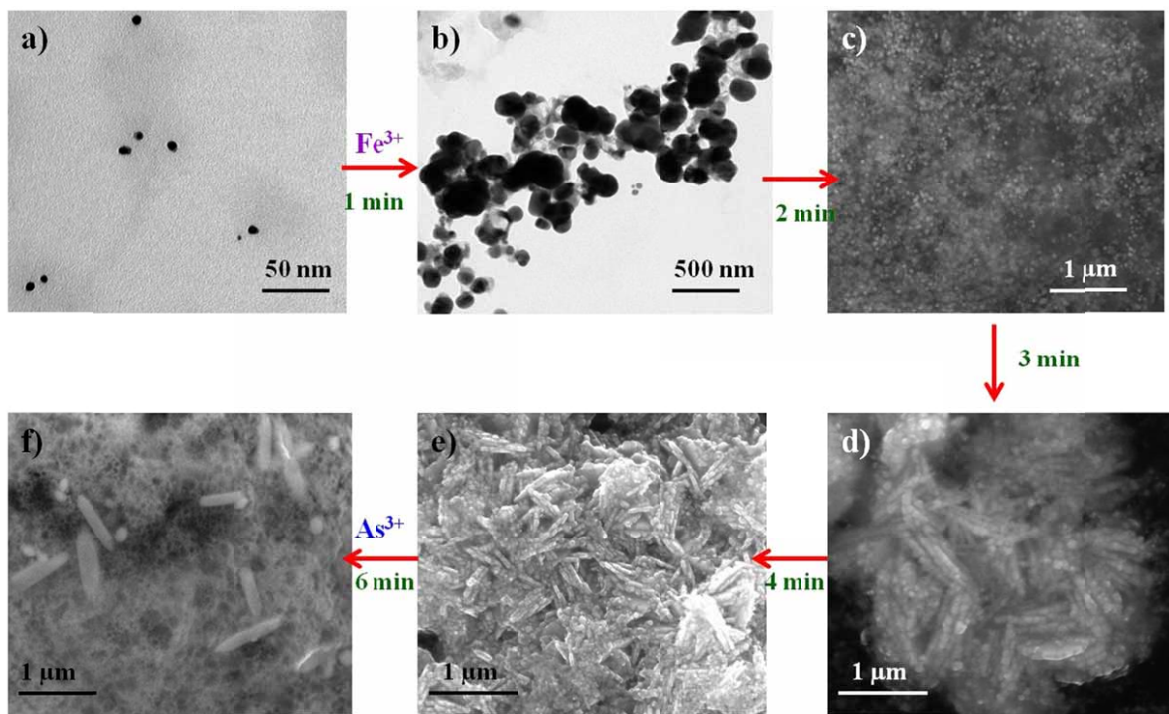


Fig. S24 TEM (a and b) and SEM (c-f) images showing the aggregation and disaggregation of AuNP1 in presence of Fe^{3+} (10^{-6} M) and As^{3+} (10^{-3} M) ions.

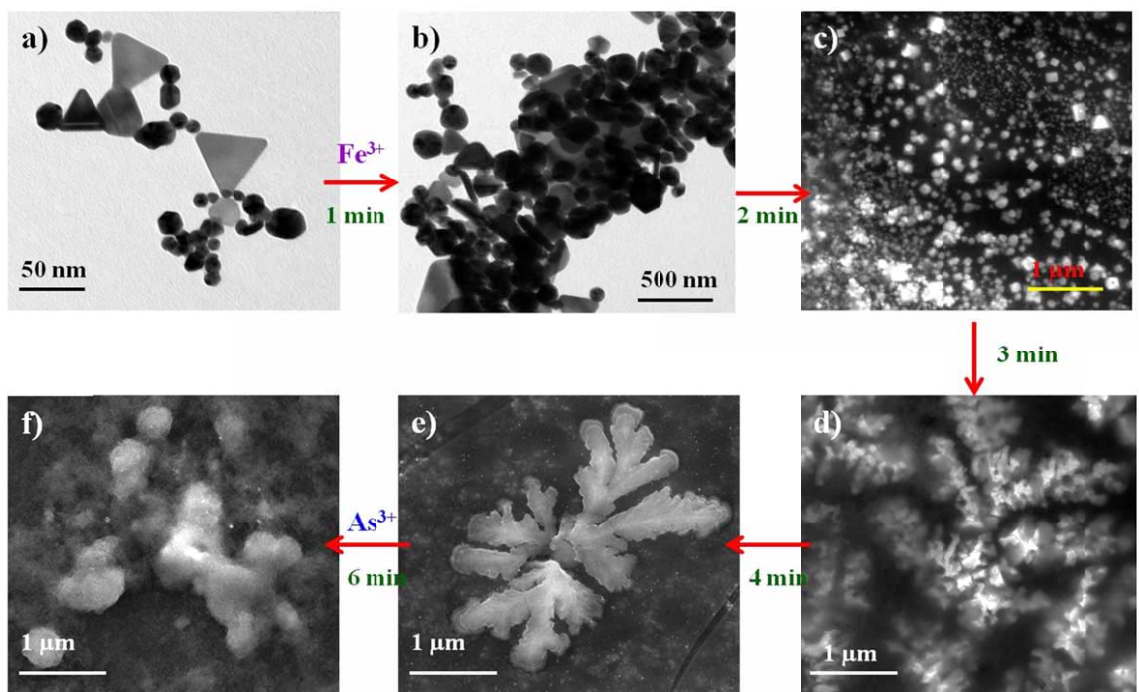


Fig. S25 TEM (a and b) and SEM (c-f) images showing the aggregation and disaggregation of AuNP2 in presence of Fe^{3+} (10^{-6} M) and As^{3+} (10^{-3} M) ions.

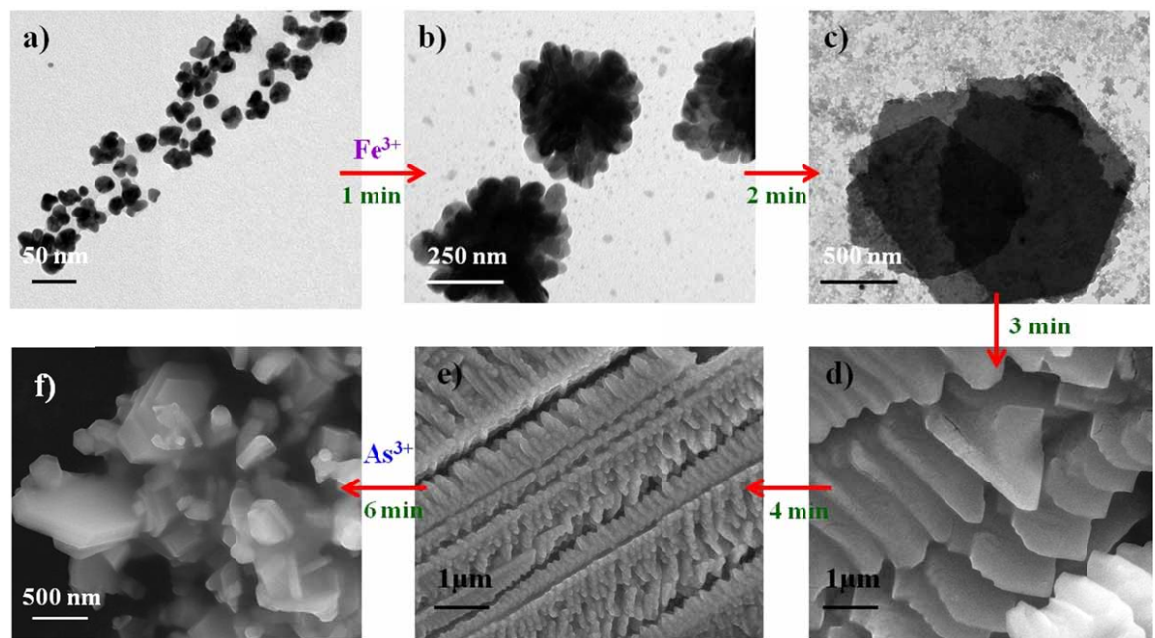


Fig. S26 TEM (a and b) and SEM (c-f) images showing the aggregation and disaggregation of AuNP3 in presence of Fe^{3+} (10^{-6} M) and As^{3+} (10^{-3} M) ions.

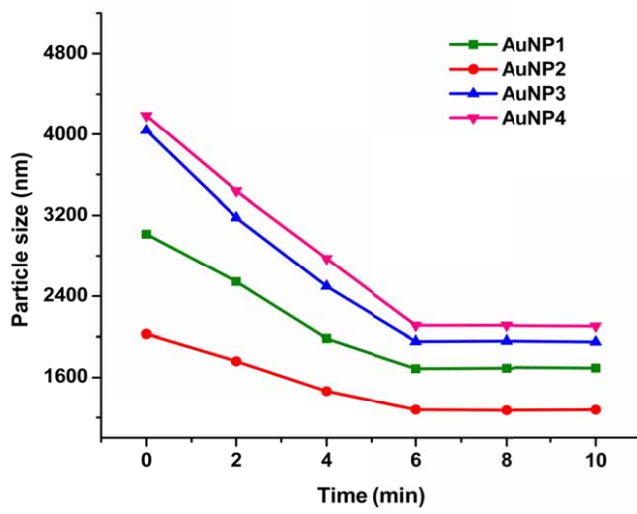


Fig. S27 Time dependent aggregation and change in particle size of AuNPs – Fe system upon addition of 10^{-3} M As^{3+} ions by DLS measurement.

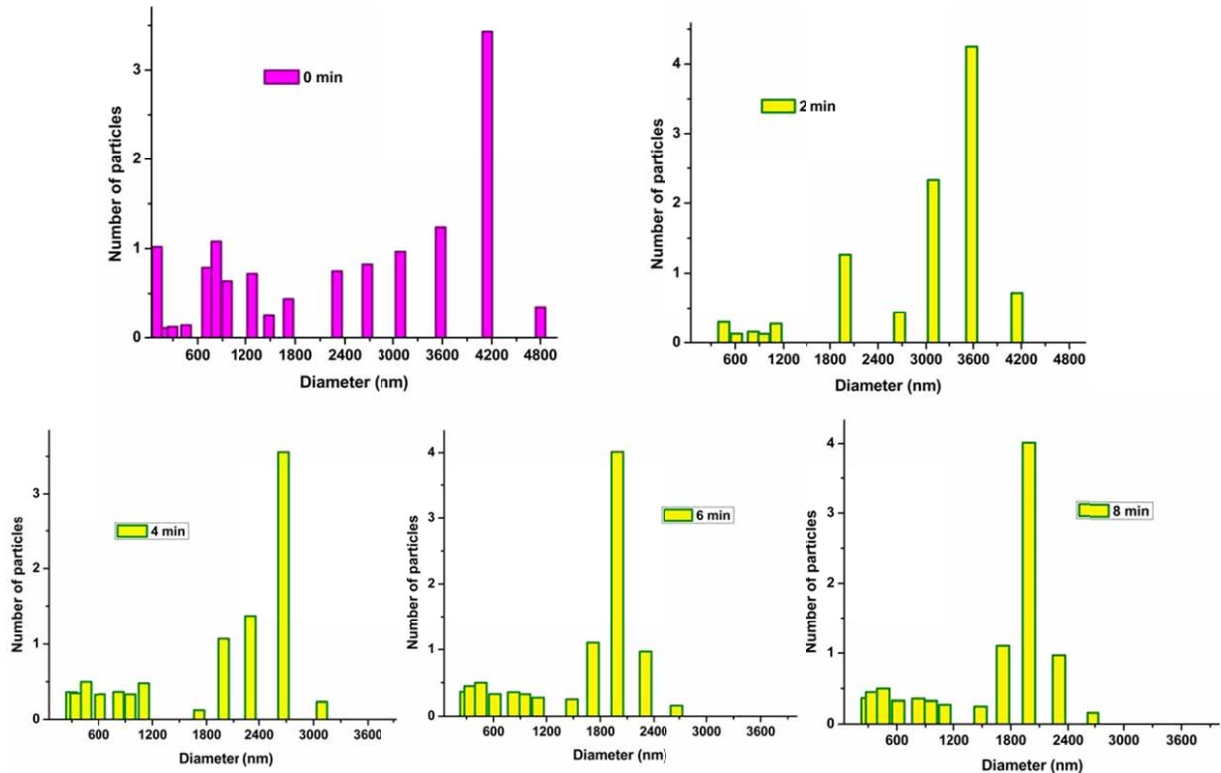


Fig. S28 Time dependent aggregation and change in particle size of AuNPs4 – Fe system upon addition of 10^{-3} M As^{3+} ions by DLS measurement.

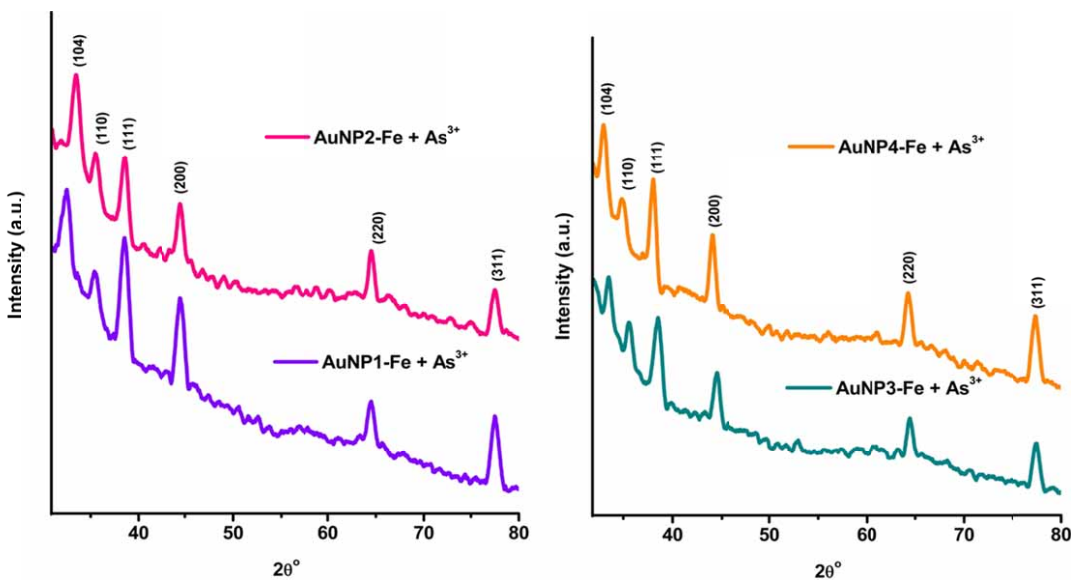


Fig. S29 XRD patterns of AuNPs-Fe system with the addition of 10^{-3} M of As^{3+} .

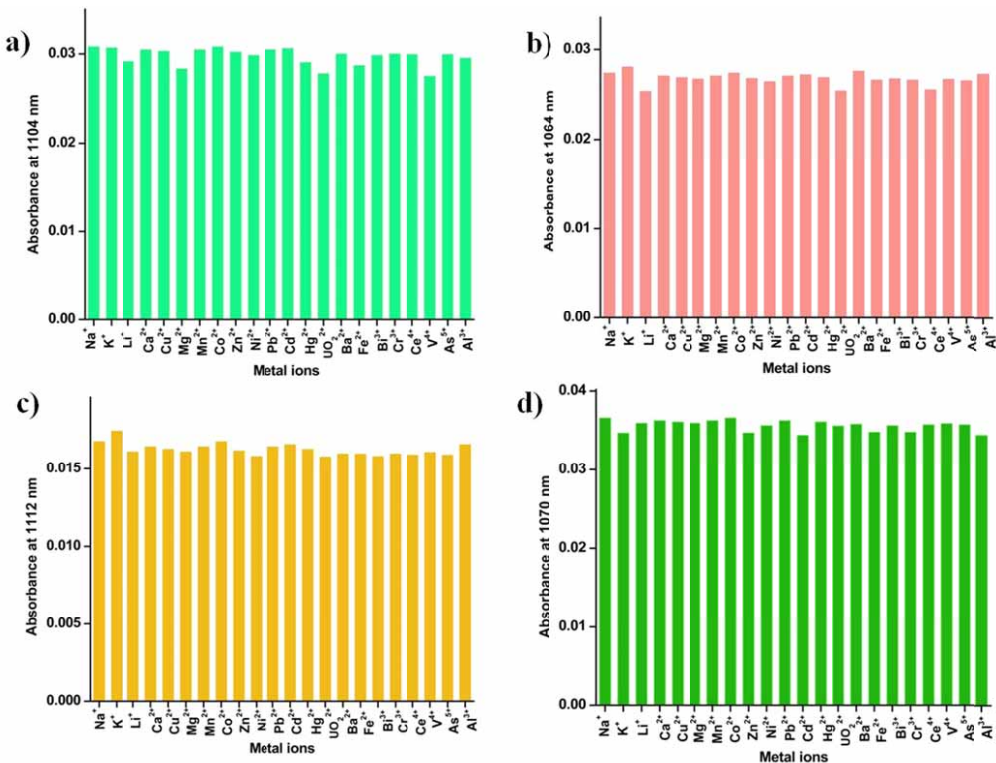


Fig. S30 Interference study of a) AuNP1-Fe b) AuNP2-Fe c) AuNP3-Fe d) AuNP4-Fe with As^{3+} in the presence of other metal ions.

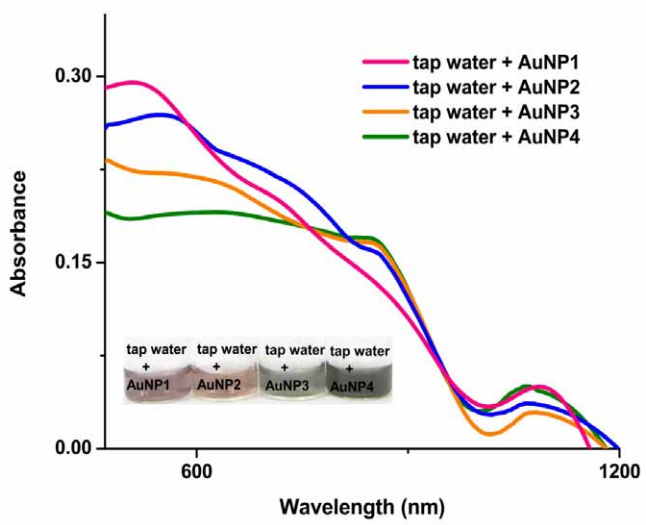


Fig. S31 UV-vis absorption spectral response of four different AuNPs system upon addition of tap water.